TuijinJishu/Journal of Propulsion Technology
ISSN: 1001-4055
Vol. 44 No.4 (2023)

Processing and Characterization of NiTi Alloy Processed through Tungsten Inert Gas Welding

Afsar Hussain[1, a*], K. S. Narayana Swamy[2, b], S. Devaraj[3, c]

[1]Research scholar, School of Mechanical Engineering, REVA University, Bengaluru, India
[2]Director and Dean, School of Mechanical Engineering, REVA University, Bengaluru, India
[3]Professor, School of Mechanical Engineering, REVA University, Bengaluru, India

Abstract

This study investigates TIG welding of NiTi alloy under three different parameters, referred to as parameter 1, parameter 2, and parameter 3, while maintaining constant welding conditions. Investigations include optical micrographs, EDAX analysis, micro-Vickers hardness testing, and yield and tensile strength evaluations.The optical micrographs unveiled diverse surface topographies, including fine secondary phase distribution, equiaxed and coarse grains, as well as dendritic structures, contingent upon the solidification process. EDAX reports confirmed the presence of crucial elements, Ni and Ti, while reassuringly revealing the absence of oxide formation during welding. Notably, micro-Vickers hardness testing demonstrated significant variations in hardness values attributed to the uniform distribution of secondary phases within the matrix. The most striking observation of 40% increase in the 0.2% yield strength and a 10% enhancement in ultimate tensile strength as the welding current parameter was elevated from 50 A to 100 A. This remarkable improvement in strength can be primarily attributed to microstructural modifications across different zones and impact of welding current on mechanical properties. These findings underscore crucial role of welding parameters in shaping the microstructure and mechanical performance of NiTi alloy, providing valuable insights for optimizing TIG welding processes in various applications, from aerospace to medical device manufacturing.

Keywords:*NiTi alloy, TIG welding, Microstructure, Micro Vickers Hardness, Tensile properties*

Introduction

Nickel Titanium (NiTi) alloy, renowned high-temperature properties, corrosion resistance, and fatigue strength, holds a pivotal role in diverse engineering and biomaterial applications, spanning from industrial machinery to medical devices [1-4]. Recent years have witnessed growing interest in the fusion-based welding of NiTi shape memory alloy, spurred by its potential across various industries. However, as we delve into the realm of NiTi alloy

welding, a conspicuous research gap emerges - the impact of welding parameters on microstructure and mechanical properties remains an underexplored frontier.Traditional fusion-based welding processes, particularly Tungsten Inert Gas (TIG) welding, are recognized for their precision and versatility. Nevertheless, the nuanced interplay between welding parameters, microstructural characteristics, and resulting mechanical properties in NiTi alloys remains inadequately studied. Prior research has often focused on joining NiTi alloy wires and thin sheets, leaving a dearth of knowledge regarding the application of this material in structural contexts [7-10].

Moreover, the welding of NiTi alloy presents unique challenges. This alloy's high reactivity at elevated temperatures necessitates meticulous control over environmental factors such as oxygen and hydrogen exposure to prevent oxidation [9]. Additionally, the welding process can induce transformations in the alloy's super plasticity and shape memory effects [15]. Understanding how these intricate factors are influenced by welding parameters is crucial for harnessing the full potential of NiTi alloy in both biomedical and civil engineering applications.

To address this research gap, this study focuses on TIG welding of NiTi alloy under three different welding current parameters, labelled as parameter-1, parameter-2, and parameter-3, while keeping all other welding conditions constant. Through a comprehensive analysis encompassing microstructural examinations, EDAX reports, micro-Vickers hardness testing, and evaluations of yield strength and ultimate tensile strength, we aim to unravel the intricate relationship between welding parameters, microstructure, and mechanical properties in NiTi alloy. The insights gained from this study will not only enhance our understanding of NiTi alloy welding but also pave the way for optimized welding processes with broad applications in engineering and beyond.

Experimental work

The research involved TIG welding of 3 mm thick NiTi alloy plates using three different welding parameters. Initially, 40x40 mm NiTi samples were obtained from the as-received material, which were then prepared for butt welding. To ensure the creation of high-quality welded joints, the welding samples underwent a thorough cleaning process using a cleaning agent to remove surface impurities. TIG welding was conducted using our in-house welding equipment, complete with a welded chamber and inert gas shielding to supply Ar inert gas during the welding process. To enhance mechanical properties, TIG welding was carried out in the rolling direction [16]. The welding speed was maintained at 0.2 m/min, with gas protection rates set at 15 l/min on the weld face and 8 l/min at the root. Weld speed was meticulously controlled using an Instek function generator, while sensors were strategically placed to prevent any damage to the weld structure during the welding process. Throughout welding, the molten material effectively penetrated the weld joint while minimizing surface oxidation. The surface of the samples was examined using an Olympus CX40 optical metallurgical microscope at various magnifications, allowing for microstructure analysis at different points on the base metal, heat-affected zone (HAZ), and the interface.

The arc currents of 50, 75, and 100 A were employed for TIG welding of NiTi alloy and are referred to as parameters 1, 2, and 3, respectively, in this article. All other welding parameters for TIG welding remained constant, as indicated in Table 1 below. SEM micrographs and EDAX analysis were conducted using the Oxford Instruments INCAX Sight EDS system and the FEI Quanta 400 FEG ESM equipped with the EDAX Genesis X4M EDS analyzer. Microhardness testing was performed using the Mitutoyo HM-112 microhardness tester, applying a load of 100 g for a dwell time of 10 s. Indentations were made at various locations on the samples, including the base metal, heat-affected zone (HAZ), and interfaces of the welded joints. Precision cutting samples for microstructure analysis, microhardness testing, and tensile testing, all of which were obtained from butt-welded NiTi joints were prepared.

Uniaxial tensile tests for all TIG-welded samples were conducted using the Autograph Shimadzu model, equipped with a 50 kN load cell. Yield strength and ultimate tensile strength of the welded samples were calculated after conducting the tensile test at a strain rate of 1 mm/min. The same strain rate was employed for all tensile tests on the welded samples.

Table 1 Welding parameters employed of TIG welding of NiTi alloy

TIG WELDING PARAMETERS								
Parameter No	**Arc Current (A)**	**Arc Voltage (V)**	**Welding speed (mm/min)**	**Gas flow rate (lit/min)**	**Electrode diameter (mm)**	**Electrode tip angle**	**Electrode distance (mm)**	**Shield gas**
Parameter 1	50	45	500	17	3.2	45 DEG	3	Argon
Parameter 2	75	45	500	17	3.2	46 DEG	3	Argon
Parameter 3	100	45	500	17	3.2	47 DEG	3	Argon

Results and Discussion

Microscopic Studies

The optical micrographs of TIG welding of NiTi alloy employing parameter-1 for welding are presented in Figure 1. Micrographs of welding parameter-1 were captured at various zones, including the base metal, welded zone, heat-affected zone, and the fusion zone. Figure 1(a) illustrates the uniform distribution of equiaxed secondary phases. This even distribution of secondary phases within the matrix significantly enhances the mechanical properties of the alloy. Fusion and heat-affected zones are highlighted in Figure 1(b), with the equiaxed distribution of secondary phases observed in the fusion zone. Notably, the micrograph reveals clear grain growth in the heat-affected zone. Figure 1(c) portrays the microstructure of the base metal in the welded joint, showing regions of the alloy with elongated and dendritic microstructures. A high-magnification image of the fusion zone is displayed in Figure 1(d), demonstrating directional solidification of the weld metal.

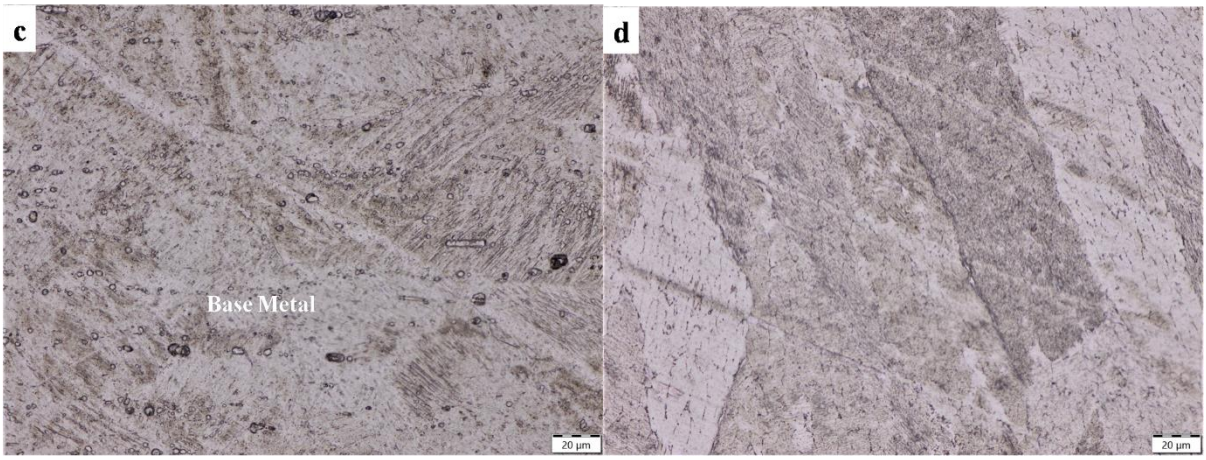

Fig.1 Optical images of parameter-1 of NiTi TIG welded alloy (a) distribution of secondary phase, (b) different welded zones, (c) microstructure base metal and (d) High magnified image welded zone.

The micrographs of the NiTi TIG-welded alloy for welding parameter-2 are depicted in Figure 2. Fine micron-sized equiaxed grains, as shown in Figure 2(a), are evident in the base metal of the welded joint. Figure 2(b) displays the interface between the base metal and the heat-affected zone. In the base metal, equiaxed grains are observed, while the heat-affected zone exhibits a lamellar and dendritic structure. Notably, the welding zone between these two phases displays a secure bond without any signs of oxidation or defects. Visible grain growth in the heat-affected zone is evident in Figure 2(c). This grain growth occurs in the heat-affected zone due to the presence of liquid metal, which necessitates some time for solidification. Figure 2(d) provides a higher magnification view, showing a dendritic structure. The welded NiTi alloy is subjected to high temperatures, reaching its melting point. The solidification or cooling rate at the welding zone is slow, requiring additional time for the melt to solidify.

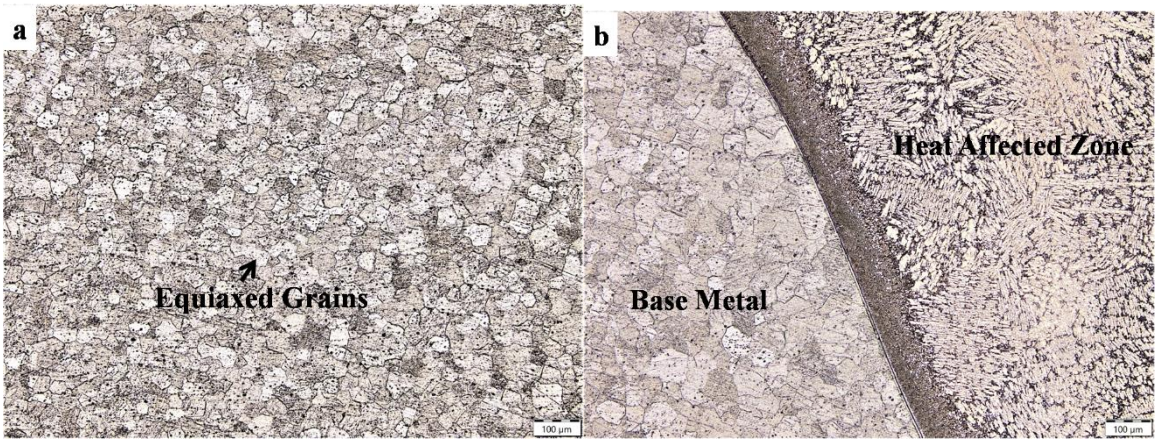

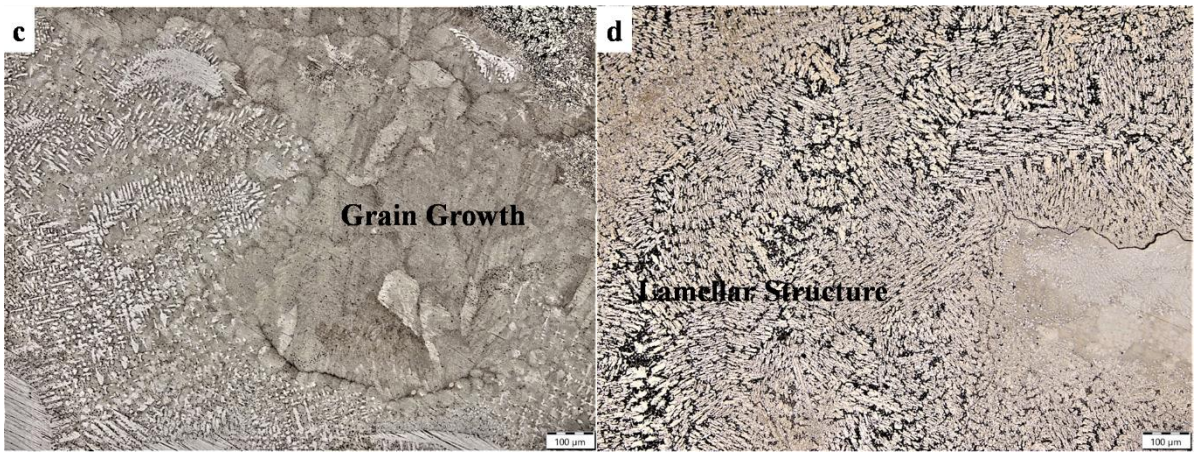

Fig. 2 Optical micrographs of parameter-2 (a) base metal, (b) different regions, (c) heat affected zone, and (d) region of lamellar structure.

Micrographs of the NiTi TIG-welded samples, using the specified welding parameters, are presented in Figure 3. Micrographs reveal varying microstructures across different zones. Figure 3(a) illustrates surface topography of base metal, providing insight into the grain arrangement within the welded joint. As the metal reaches a molten state during the welding process, it fuses together between the two zones. Figure 3(c) highlights the presence of secondary phase spreading within the matrix, though the distribution is not uniform. The TIG-welded alloy exhibits diverse shapes and sizes of secondary phases, ranging from equiaxed to elongated, coarse, and dendritic structures. The shape and size of these secondary phases are influenced by the cooling rate, with smaller portions cooling more rapidly compared to larger ones, where the cooling rate is relatively slower.

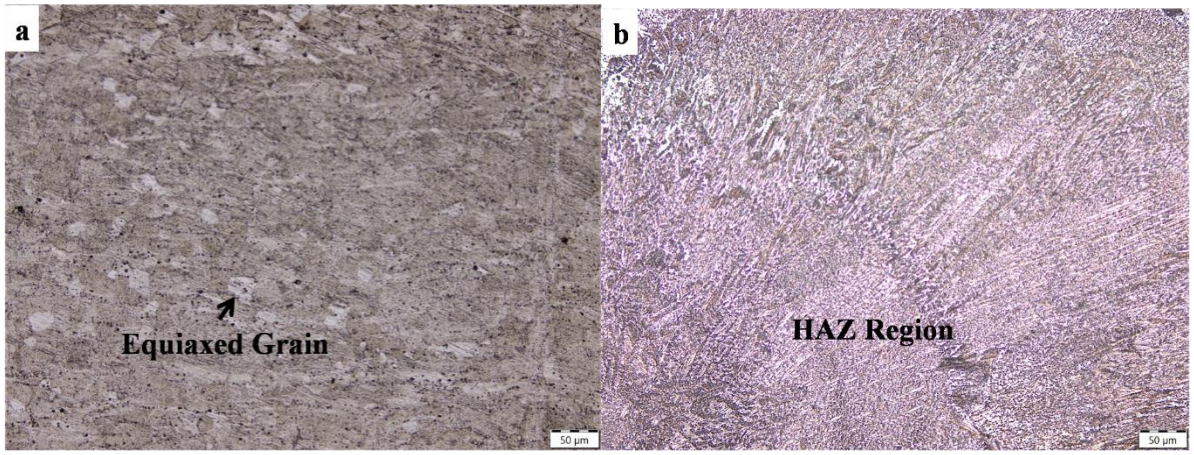

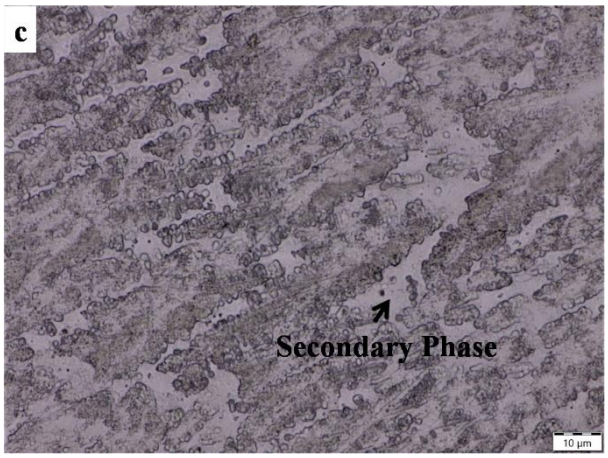

Fig. 3 Optical micrographs of parameter 3 (a) base metal, (b) heat affected zone and (c) fusion zone of high magnified image.

EDAX reports for TIG welding under parameter-1, parameter-2, and parameter-3 are presented in Fig 4. EDAX analysis was conducted at various locations for all three parameters to confirm the elemental phases present. The EDAX reports confirm that the welded joint comprises Ni and Ti at different weight percentages, with distinct peaks indicating these percentages shown as insets in the micrographs. The red-colored boxes in the figures highlight different regions of the samples where EDAX analysis was performed. Furthermore, the micrographs reveal the absence of inclusions or porosity in the welded alloy. Additionally, there is no evidence of oxide formation in the welding zone during the welding process.

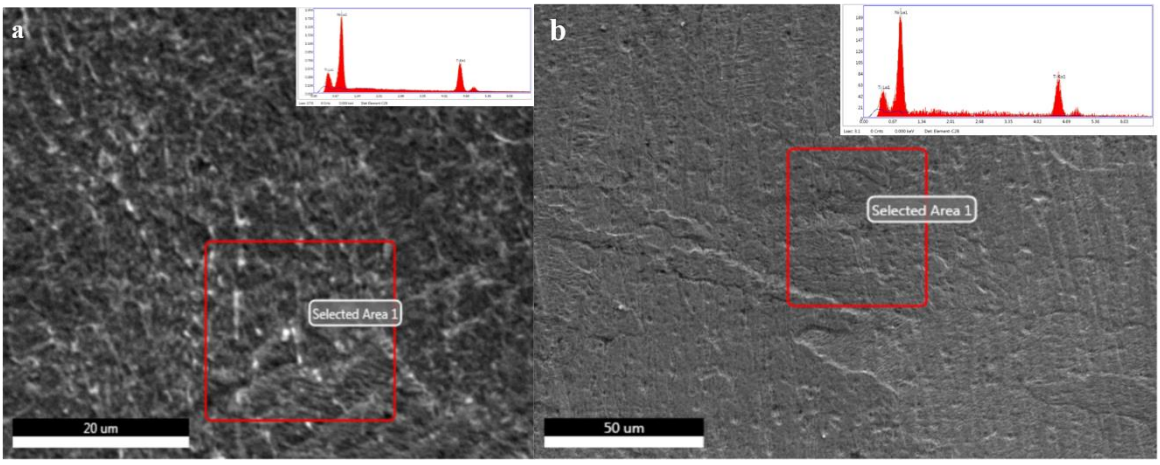

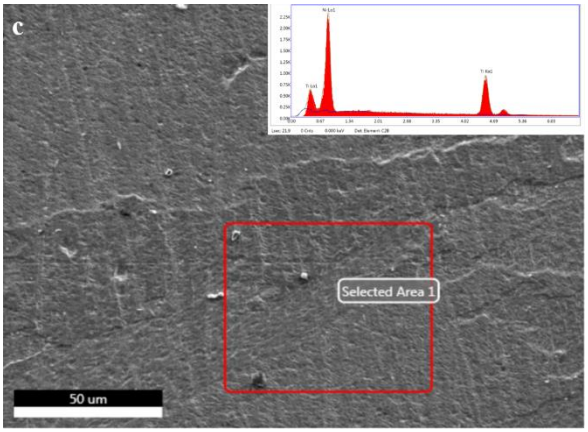

Fig.4 SEM EDAX reports of (a) parameter-1, (b) parameter-2 and (c) parameter-3

Mechanical properties

An average microhardness of TIG-welded NiTi alloy in three different zones, namely the BM, HAZ, and WZ, for parameter-1, is measured as 303 HV1, 267 HV1, and 257 HV1, respectively. It's notable that the base metal exhibits higher hardness compared to HAZ and WZ of the TIG-welded NiTi alloy joint. These variations in hardness can be attributed to the differences in microstructures reported in Figures 1(a) to 1(c), where the cooling rate in HAZ and WZ slower than in base metal.

For parameter 2, the microhardness of TIG-welded NiTi alloy in different zones (base metal, heat-affected zone, and welding zone) is reported to be 352 HV1, 279 HV1, and 237 HV1, respectively. Interestingly, for parameter 2, the hardness decreases from the base metal through the heat affected zone to the weld. These hardness changes can be influenced by the microstructural differences shown in Figures 2(a)–2(c).

Finally, for parameter-3, microhardness values for BM, HAZ, and welding zone are 318 HV1, 258 HV1, and 237 HV1, respectively. The variations in hardness values for parameter-3 correspond to the microstructure variations seen in Figures 3(a) to 3(c).

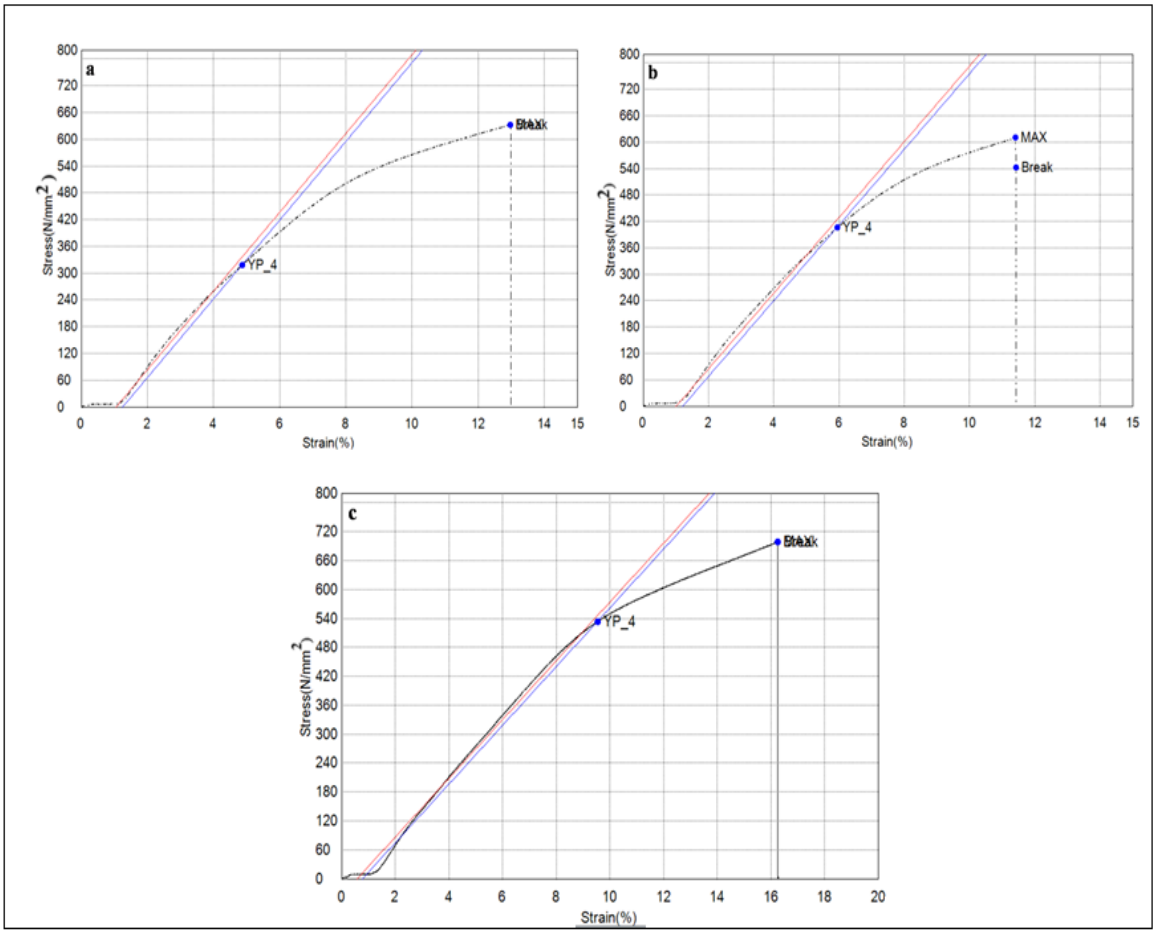

Fig. 5 Stress and strain diagram of NiTi TIG welded (a) parameter-1, (b) parameter-2 and (c) parameter-3.

The 0.2% yield strengths of TIG-welded NiTi alloy for parameter-1, parameter-2, and parameter-3 are 318 MPa, 406 MPa, and 534 MPa, respectively. Similarly, the ultimate tensile strengths for parameter-1, parameter-2, and parameter-3 are 633 MPa, 610 MPa, and 699 MPa. Notably, the 0.2% yield strength exhibits a substantial increase from 318 MPa to 534 MPa as the TIG welding parameter changes from parameter-1 to parameter-3. Increasing the welding current from 50 A (parameter-1) to 75 A (parameter-2) results in a rise in the 0.2% yield strength from 318 MPa to 406 MPa. Furthermore, a further increase in TIG welding current to 100 A (parameter-3) leads to an elevated 0.2% yield strength of 534 MPa. The experimental stress-strain diagrams support this observation, demonstrating a significant increase in the 0.2% yield strength as the welding current is escalated from A similar trend is observed for the tensile strength as the welding current varies from 50 A to 75 A to 100 A over parameter 1, parameter 2, and parameter 3. When the welding current increases from 50 A to 75 A (parameter 1 to parameter 2), the tensile strength decreases from 633 MPa to 610 MPa, and then when the welding current increases from 75 A to 100 A, the tensile strength increases from 610 MPa to 699 MPa (parameter-2 to parameter-3). Therefore, welding current parameters play an important role in improving the ultimate tensile strength of TIG-

welded NiTi alloys.Additionally, it is evident that microstructural variations, as indicated in Figures 1, 2, and 3, serve as the primary determinants in the enhancement of mechanical properties, including hardness, yield strength, and ultimate tensile strength.

Practical Implications and Future Directions

The findings of this study hold significant practical implications for various industries, particularly in the fields of aerospace, automotive, medical device manufacturing, and beyond. Understanding the intricate relationship between welding parameters, microstructure, and mechanical properties in NiTi alloy opens doors for optimizing welding processes. Engineers and materials scientists can harness this knowledge to design and fabricate high-performance components and structures, benefitting from NiTi alloy's unique properties. For instance, in the aerospace sector, the enhanced mechanical properties resulting from controlled welding parameters can lead to the development of lighter, more durable aircraft components. Similarly, in the medical field, where NiTi alloys are widely used in devices like stents and orthopedic implants, this research can pave the way for improved and more reliable medical devices.

As for future directions, there is a wealth of possibilities to explore. Further investigations could delve into the finer nuances of welding parameters, seeking to optimize them for specific applications and industries. Additionally, research on the long-term durability and reliability of NiTi alloy components produced using these optimized parameters is paramount. Moreover, the study of other advanced welding techniques and their applicability to NiTi alloys, such as laser welding or electron beam welding, presents exciting avenues for research. Finally, interdisciplinary collaboration with experts in fields like material science, metallurgy, and biomedical engineering can facilitate the development of novel NiTi alloy-based solutions with broader applications in emerging technologies and healthcare. Overall, this study lays a robust foundation for advancing the utilization of NiTi alloy in diverse industrial contexts and serves as an invitation for continued exploration and innovation.

Conclusions

In this study, we embarked on a systematic exploration of TIG welding of NiTi alloy, delving into the effects of varying welding parameters on microstructure and mechanical properties. Our findings shed light on the intricate relationship between welding current parameters, microstructural characteristics, and the resultant mechanical behavior of NiTi alloy.

Firstly, our optical micrographs unveiled a spectrum of surface topographies, ranging from fine secondary phase distribution to equiaxed and coarse grains, along with dendritic structures. These observations align with previous studies, emphasizing the importance of welding parameters in shaping microstructural features.EDAX analysis not only confirmed the presence of critical elements, Ni and Ti but also highlighted the absence of oxide formation during welding. Significant variations in micro-Vickers hardness values were observed, corresponding to changes in welding current parameters. Results align with

research, underscoring the influence of welding parameters on the uniform distribution of secondary phases within the matrix.

Most notably, the 0.2% yield strength exhibited a substantial 40% increase, and the ultimate tensile strength rose by10% as the welding current parameter was escalated from 50 A to 100 A. These findings are consistent with the work of further highlighting the pivotal role of welding parameters in enhancing the mechanical performance of NiTi alloy.

The study objectives were twofold: first, to comprehensively investigate the influence of welding parameters on microstructure and mechanical properties in NiTi alloy, and second, to bridge the research gap in understanding the application of NiTi alloy in structural contexts. Through our systematic examination, we have achieved both objectives.

Research outcome is not only advancing the fundamental understanding of NiTi alloy welding but also underscores its potential in various engineering applications, from aerospace to medical devices. The insights gained here provide a valuable foundation for optimizing TIG welding processes and offer a platform for future research endeavours in this domain.

References

[1] Kimura K and Tobushi H 1996, TIG welding and shape memory effect of TiNi shape memory alloy, Journal of intelligent material systems and structures, 7, 646-655.
[2] Tuissi A, Besseghini S, Ranucci T and Squatrito F 1999 Effect of Nd-YAG laser welding on the functional properties of the Ni–49.6 at.% Ti Mater. Sci. Eng. A 273–275 813–7.
[3] Falvo A, Furgiuele F M and Maletta C 2005 Laser welding of a NiTi alloy: mechanical and shape memory behavior Mater. Sci. Eng. A 412 235–40.
[4] Yan X J, Yang D Z and Qi M 2006 Rotating–bending fatigue of a laser-welded superelastic NiTi alloy wire Mater. Charact. 57 58–63.
[5] Gugel H, Schuermann A and Theisen W2008 Laser welding of NiTi wires Mater. Sci. Eng. A 481–482 668–71.
[6] Chan C W, Man H C and Yue T M 2011 Effects of process parameters upon the shape memory and pseudo-elasticbehaviors of laser-welded NiTi thin foil Metall. Mater.Trans. A 42 2264–70.
[7] Hsu Y, Wang Y, Wu S and Chen C 2001 Effect of CO2 laser welding on the shape-memory and corrosion characteristics of TiNi alloys Metall. Mater. Trans. A 32A 569–76.
[8] Falvo, Furgiuele F M and Maletta C 2008 Functional behavior of a NiTi-welded joint: two-way shape memory effect Mater. Sci. Eng. A 481–482 647–50.
[9] Oliveira J P, Braz Fernandes F M, Schell N and Miranda R M2015 Shape memory effect of laser welded NiTi platesFunct. Mater. Lett. 8 1550069.
[10] Oliveira J P, Miranda R M, Schell N and Braz Fernandes F M2016 High strain and long duration cycling behavior of laserwelded NiTi sheets Int. J. Fatigue 83 195–200.
[11] Pires J N, Loureiro A and Bölmsjo G 2006 Welding Robots: Technology, System Issues and Application. Journal of Intelligent Materials Systems and Structures, 17(11), 962–972.

[12] Fox J, Hahnlen R and Dapino M J 2012 Fusion welding ofnickel-titanium and 304 stainless steel tubes: II. Tungsteninert gas welding J. Intel. Mat. Syst. Str. 24 962–72.
[13] Ikai A, Kimura K and Tobushi H 1996 TIG welding and shapememory effect of TiNi shape memory alloy J. Intel. Mat.Syst. Str. 7 646–55.
[14] Oliveira1J P, BarbosaD, Braz FernandesF M and MirandaR M, 2016, Tungsten inert gas (TIG) welding of Ni-rich NiTi plates: functional behavior, Smart Mater. Struct. 25 1-7.
[15] Jani J M, Leary M, Subic A and Gibson M A 2014 A review ofshape memory alloy research, applications and opportunitiesMater & Design 56 1078–113.
[16] Vieira L, Braz Fernandes F M, Miranda R M, Silva R J C,Quintino L, Cuesta A and Ocaña J L 2011 Mechanicalbehavior of Nd: YAG laser welded superelastic NiTiMater. Sci. Eng. A 528 5560–5.